



Provided by the author(s) and University of Galway in accordance with publisher policies. Please cite the published version when available.

Title	Secondary comminution of wood pellets in power plant and laboratory-scale mills
Author(s)	Trubetskaya, Anna; Poyraz, Yunus; Weber, Roman; Wadenbäck, Johan
Publication Date	2017-03-14
Publication Information	Trubetskaya, A., Poyraz, Y., Weber, R., & Wadenbäck, J. (2017). Secondary comminution of wood pellets in power plant and laboratory-scale mills. <i>Fuel Processing Technology</i> , 160, 216-227. doi: <a href="https://doi.org/10.1016/j.fuproc.2017.02.023">https://doi.org/10.1016/j.fuproc.2017.02.023</a>
Publisher	Elsevier
Link to publisher's version	<a href="https://doi.org/10.1016/j.fuproc.2017.02.023">https://doi.org/10.1016/j.fuproc.2017.02.023</a>
Item record	<a href="http://hdl.handle.net/10379/7358">http://hdl.handle.net/10379/7358</a>
DOI	<a href="http://dx.doi.org/10.1016/j.fuproc.2017.02.023">http://dx.doi.org/10.1016/j.fuproc.2017.02.023</a>

Downloaded 2024-05-12T07:13:53Z

Some rights reserved. For more information, please see the item record link above.



# Secondary comminution of wood pellets in power plant and laboratory-scale mills

Anna Trubetskaya<sup>a,\*</sup>, Yunus Poyraz<sup>b</sup>, Roman Weber<sup>b</sup>, Johan Wadenbäck<sup>c</sup>

<sup>a</sup>*Department of Energy Engineering, Luleå University of Technology, 97187 Luleå, Sweden*

<sup>b</sup>*Institute of Energy Processes Engineering and Fuel Technology, Clausthal University of Technology, 38678 Clausthal-Zellerfeld, Germany*

<sup>c</sup>*Amager power plant, HOFOR A/S, Kraftværkvej 37, 2300 Copenhagen S, Denmark*

---

## Abstract

This study aims to determine the influence of mill type and pellet wood composition on particle size and shape of milled wood. The size and shape characteristics of pellets comminuted using power plant-scale roller- and hammer mills were compared with those obtained by using a laboratory-scale roller mill. A 2D dynamic imaging device was used for particle characterization. It was shown that mill type has a significant impact on particle size but an almost negligible effect on the shape of milled wood. Comminution in the pilot plant using a Loesche roller mill requires less energy than using a hammer mill, but generates a larger fraction of coarse particles. The laboratory-scale roller mill provides comparable results with the power plant roller mill with respect to particle size and shape.

*Keywords:* pellets, hammer mill, roller mill, particle size, shape

---

## Nomenclature

---

\*Corresponding author. anna.trubetskaya@ltu.se

$A$	Particle area (m <sup>2</sup> )	$q_3$	Frequency particle distribution, based on volume (% mm <sup>-1</sup> )
$AR$	Aspect ratio		
$A_{convex}$	Particle convex area (m <sup>2</sup> )		
$A_{real}$	Particle projection area (m <sup>2</sup> )	$r_1, r_2$	Distances from the area center to the particle edges (m)
$b$	Particle width (m)	$SPHT$	Circularity (Sphericity)
$Conv$	Convexity	$Symm$	Symmetry
$d$	Diameter (m)	$V$	Volume (m <sup>3</sup> )
$l$	Particle length (m)	$x_{Fe,max}$	Feret maximum diameter (m)
$m$	Number of size classes	$x_{Ma,min}$	Martin minimum diameter (m)
$P$	Perimeter of a particle projection (m)		
$\bar{q}_3$	Histogram (% mm <sup>-1</sup> )		
$Q_3$	Cumulative particle distribution, based on volume (% mm <sup>-1</sup> )		
		<b>Subscripts</b>	
		$i$	Number of the size class with upper limit $x_i$

## 1. Introduction

1 Biomass firing is used for power generation and is considered as an im-  
2 portant step in the reduction of greenhouse gas emissions. The anthropogenic  
3 CO<sub>2</sub> emissions can be decreased by the substitution of biomass in pulverized  
4 combustion due to the lower regeneration time of biomass compared to bitu-

5 minous coal. Thus, CO<sub>2</sub> released using biofuels will be reconsumed faster by  
6 other plants via photosynthesis than the time needed to regenerate coal. The  
7 milling process is a necessary step in suspension fuel firing [1]. Size reduction  
8 improves conversion processes due to the creation of larger reactive surface  
9 areas [2, 3]. Biomass is due to its fibrous structure difficult to mill. An in-  
10 creased energy input into biomass comminution affects the total efficiency of  
11 power plants, and often causes problems with flame stability and burnout  
12 when large particles remain after milling.

13 The common method for preparing biomass for suspension firing is to  
14 pelletize lignocellulosic materials, and then pulverize the biomass pellets us-  
15 ing coal roller mills [4]. A number of studies [3, 5–10] have investigated the  
16 influence of mill type on both the particle size and shape. Momeni [5] showed  
17 that comminuting woody pellets in hammer and roller mills produced signif-  
18 icantly different sized particles. In other investigations [6, 8], higher fractions  
19 of fine particles were obtained after comminution in a hammer mill compared  
20 to milling using a knife mill. In agreement with this observation, the energy  
21 consumption of the knife mill was found in all cases to be smaller than that  
22 of the hammer mill [7, 8]. The feedstock type (hardwood, straw, corn cobs  
23 and corn stover) affected the energy consumption of the hammer and disk  
24 mills [9]. The energy consumption for the comminution of dry pellets was  
25 lower for the hammer mill than for the disk mill, and the particle size dis-  
26 tribution was broader with larger particle aspect ratios after comminution  
27 in the hammer mill [10]. In addition, it was reported that a high moisture  
28 content (> 20 %) increased the specific energy consumption by 50 % [10]. It  
29 appeared that different feedstocks (switchgrass, corn and soybean) showed

30 differences in the particle size and shape during comminution and generated  
31 particles with various morphological properties [11]. Previous investigations  
32 of biomass comminution demonstrate disagreements in terms of the effect  
33 that mill and feedstock type have on particle shape. Bond [12] and Hey-  
34 wood [13] reported that fuel type has a stronger influence on the particle  
35 shape than mill type, whereas Rose [14] showed that mill type mainly affects  
36 particle shape. Generally, little is known about the effect of mill type on  
37 particle shape and size when lignocellulosic materials are milled.

38 In this study, the impacts of mill and feedstock type on particle size and  
39 shape were investigated. Wood pellets are comminuted using a laboratory-  
40 scale roller mill, a laboratory-scale hammer mill, and power plant-scale Loesche  
41 roller mills. Particle size and shape of milled pellets were characterized us-  
42 ing sieving and 2D dynamic imaging analysis. The objective of this study  
43 was to gain knowledge concerning the impact of mill type, fuel type, and  
44 pelletization method on both particle size and shape of milled biomass.

## 45 **2. Materials and methods**

46 Raw pellets, without additives or binding agents, were provided by the  
47 companies LatGran (Latvia) and Heatlets (Estonia). The pellets were pro-  
48 duced in the process shown in Figure 1. Wood logs with diameters of 5-60 cm  
49 and length of 3-4 m were initially dried, and then shredded in a mobile shred-  
50 der to 8-45 mm. The primary comminution includes the milling of wood chips  
51 to the particle size of 0.5-2 mm in diameter and 1 cm in length by a knife ring  
52 flaker and a drop feed chipper, and sawdust milling in a hammer mill to ob-  
53 tain a homogeneous and fine material below 1.5 mm in size. The sawdust

54 before being pelletized, contained 75% particles following the process de-  
55 scribed in Figure 1 and contained 25% coarse bark sawdust residues from  
56 comminution on a disk mill.

57 The pellets were produced using ring die pellet machines in which a  
58 die ring runs around fixed rollers [15]. The sawdust was added to the roller  
59 sideways and pressed through the holes of the die. The string of pressed  
60 material leaving the die was broken off into 22 mm long pellets, and then the  
61 pellets were cooled down from 90°C to room temperature for stabilization  
62 and hardening.

1. Wood logs (5-60 cm width, 3-4 m length) 2. Chips (8-45 mm)

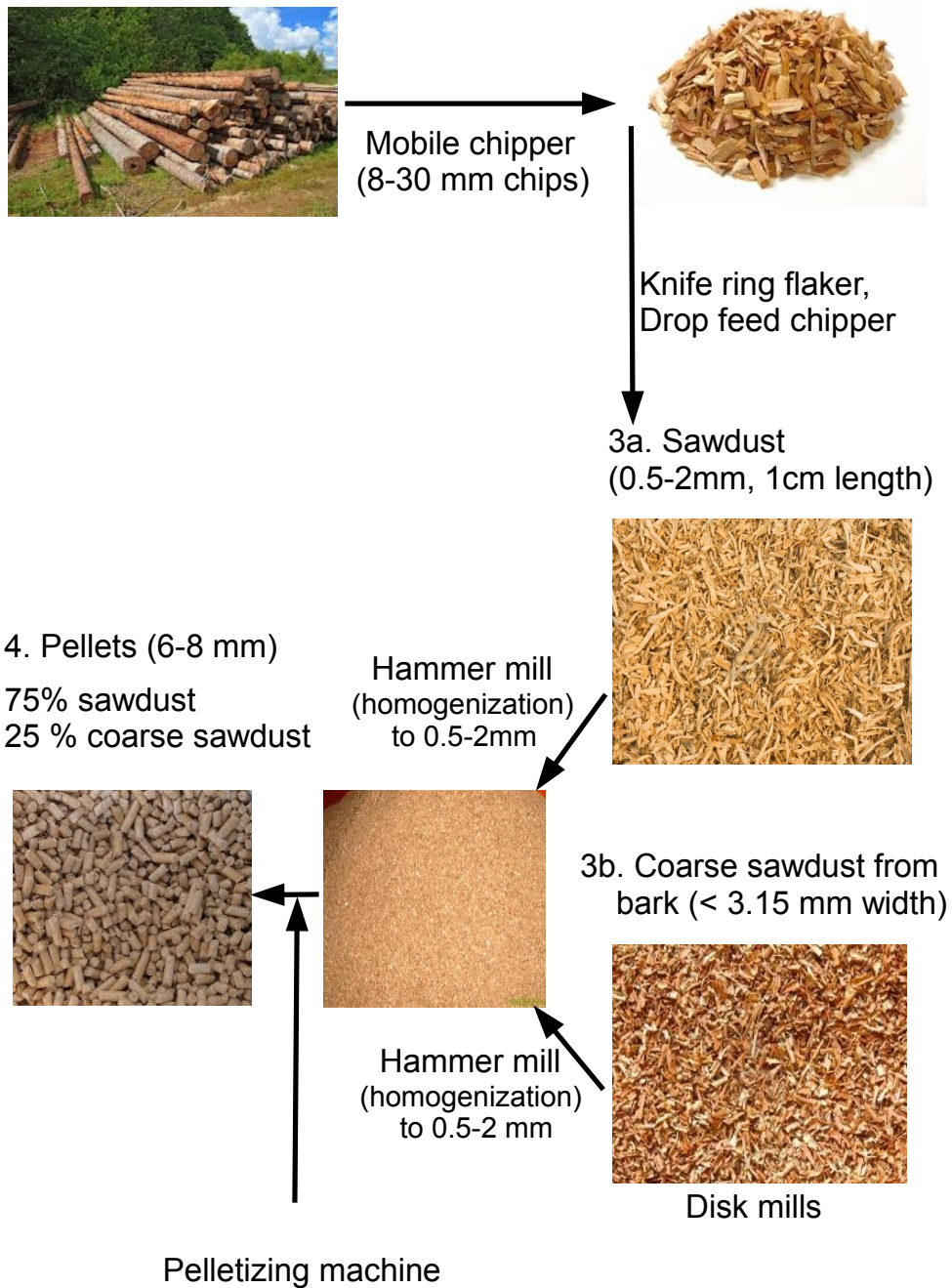


Figure 1: Wood pellets production from (1) Wood logs to (2) Chips, (3a) Sawdust combined with (3b) Coarse sawdust from bark and to (4) Pellets.

63 The pellets were transported to three power plants including Hern-  
64 ingsværket (HEV), Avedøreværket (AVV) operated by DONG Energy A/S,  
65 and Amagerværket (AMV) operated by HOFOR A/S (formally Vattenfall  
66 A/S). Secondary comminution was then carried out either in the hammer  
67 (HEV) or in the horizontal Loesche roller mills (AMV and AVV). Pulver-  
68 ized wood was sampled from the pipeline (running to the burners) through a  
69 side opening by using a vacuum cleaner or a rotorprobe. The pellets under-  
70 went additional milling in the laboratory-scale roller mill at TU Clausthal.  
71 The particle size and shape of the milled pellets were characterized by light  
72 microscopy, scanning electron microscopy (SEM), sieving and 2D dynamic  
73 imaging.

### 74 **3. Particle size and shape characterization**

75 *Light microscopy.* Light microscopy of sawdust and disintegrated pellets was  
76 conducted using a Microscope Heating Stage 1750 (Leica Microsystems, Ger-  
77 many) in order to characterize the particle shape.

78 *SEM microscopy.* SEM analysis of milled pellets was conducted using an  
79 Inspect microscope (FEI Company, USA) with a tungsten filament under  
80 high vacuum in order to obtain information on char structural properties.  
81 Prior to the analysis, milled pellet samples were coated with a thin layer of  
82 carbon (40 s, 5 mA) using a Carbon Coater 208 (Cressington, Germany) to  
83 avoid sample charging.

84 *Sample preparation.* Prior to the particle size and shape analysis, biomass  
85 samples were divided into four equal 100 mg fractions using a micro-riffler



86 PT100 (Retsch Technology, Germany).

87 *Sieving.* A vibrating sieve shaker AS 200 (Retsch Technology, Germany)  
88 comprising seven sieves ranging from 0.25 to 4 mm in opening size and a  
89 bottom pan ( $< 0.25$  mm) was used. The sieving analysis is described in  
90 EN ISO 17827-2:2016. Particles remaining on each sieve and in a bottom  
91 pan were collected and weighed using an electronic top pan balance ( $\pm 0.01$  g  
92 accuracy). The cumulative retained undersize is the mass passed from the  
93 previous sieve minus the mass retained on the current sieve [16]. Sieving was  
94 conducted for 15 min at 3 mm amplitude [17].

95 *2D dynamic imaging analysis.* The particle size and shape were measured  
96 using the CAMSIZER (Retsch Technology, Germany), designed for particles  
97 ranging from 0.03 to 30 mm in size. Particle shadows were captured by two  
98 cameras; a zoom camera, designed for the analysis of smaller particles, and a  
99 basic-camera that was able to detect larger particles. The projected area of  
100 the particle was determined using the CAMSIZER 6.3.10 software (Retsch  
101 Technology, Germany). The particle size distribution, based on volume, is  
102 represented by the  $x_{Ma,min}$  diameter. For the particle size analysis, ca. 100 mg  
103 of a dry sample was used.

104 The Martin minimal ( $x_{Ma,min}$ ) and Feret maximal ( $x_{Fe,max}$ ) diameters  
105 are suitable parameters to represent the biomass particle width and length.  
106 The Martin diameter is a characteristic length that divides the projected  
107 particle area into two equal halves [18], as shown in Figure S-1.1 of the sup-  
108 plemental material. The minimal Martin diameter ( $x_{Ma,min}$ ) is determined  
109 from the smallest Martin diameter of the particle projection [19]. The Feret

110 diameter is the distance between two tangents placed perpendicular to the  
 111 measurement direction [18], as shown in Figure S-1.2. The Feret maximal  
 112 diameter is the longest Feret diameter of all measured Feret diameters of a  
 113 particle [19].

114 In the present study, particle shape is characterized by both the spheric-  
 115 ity (SPHT) and the aspect ratio (AR). Sphericity is one of the most com-  
 116 monly used parameters to express the deviation of a two-dimensional particle  
 117 image from a sphere and is defined as

$$SPHT = \frac{4 * \pi * A}{P^2} \quad (1)$$

118 where P and A are the measured perimeter and area of a particle projection.  
 119 A particle is considered to be spherical when the value of sphericity is equal  
 120 to 1 and non-spherical when it is less than 1. The aspect ratio is defined as  
 121 the ratio of particle width ( $b = x_{Ma,min}$ ) to the particle length ( $l = x_{Fe,max}$ )  
 122 so that

$$AR = \frac{b}{l} \quad (2)$$

123 Convexity (Conv) is defined as the square root of the ratio of the real area  
 124 of a particle projection area ( $A_{real}$ ) to the convex area ( $A_{convex}$ ) so that

$$Conv = \sqrt{\frac{A_{real}}{A_{convex}}} \quad (3)$$

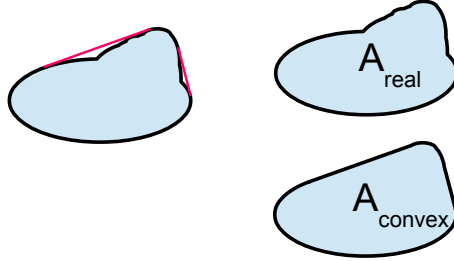


Figure 2: Definition of convexity.

125 Particle symmetry (Symm) is defined as

$$Symm = \frac{1}{2} \left( 1 + \left( \min \frac{r_1}{r_2} \right) \right) \quad (4)$$

126 where  $r_1$  and  $r_2$  are distances from the area center to the particle edges  
 127 on the same line. The center of area (C) in Figure 3 is determined by the  
 128 CAMSIZER software. Many lines are drawn in such a way that each line  
 129 passes through the center of area from particle edge to edge. The symmetry  
 130 is calculated from the smallest ratio of the resulting segments ( $r_1$  and  $r_2$ ).  
 131 For highly symmetrical particles like circles, ellipses or squares the value  
 132 for symmetry nears one. The center point divides each line in two parts.  
 133 The symmetry is equal to 0.5, if the center of the area is exactly at the  
 134 particle border. For asymmetrical particles i.e. broken beads, triangles, the  
 135 symmetry is less than one. The symmetry varies from 0 to 0.5 and  $r_1$  and  $r_2$   
 136 overlap, if the center of area is outside of a particle so that

$$\frac{r_1}{r_2} < 0 \quad (5)$$

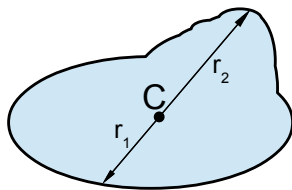


Figure 3: Definition of symmetry.

137 *Particle size distribution.* The results are presented as a cumulative particle  
 138 size distribution, based on volume. The cumulative particle size distribution  
 139 is described in EN ISO 9276-1:1998, and is defined as

$$Q_3(x_{Ma,min,m}) = \sum_{i=1}^m \bar{q}_3(x_{Ma,min,i}) \Delta x_{Ma,min,i} \quad (6)$$

140 where  $\bar{q}_3$  is the area beneath the histogram. The results of a particle size  
 141 analysis were also presented as a frequency distribution over  $x_{Ma,min}$ , based  
 142 on volume ( $q_3$ ), so that

$$q_3(x_{Ma,min}) = \frac{dQ_3(x_{Ma,min})}{dx_{Ma,min}} \quad (7)$$

143 The particle size distributions obtained from sieving and 2D dynamic imaging  
 144 were defined based on three sizes within the entire population: d10, d50,  
 145 d90. The d50 value is the median particle size within the population, with  
 146 50% of the population greater than this size, and 50% smaller than this  
 147 size. Similarly, 10% of the population is smaller than the d10 size; while  
 148 90% of the population is smaller than the d90 size [20]. All measurements  
 149 were conducted in triplicate to establish repeatability which was better than  
 150 95%, as shown in the supplemental material. The measurement inaccuracy  
 151 in sieving analysis was mainly caused by weighing errors.

#### 152 **4. Mills and sampling**

153 Mills of varying size were used in this study and are presented below in  
154 order from largest to smallest mill in terms of throughput.

155 *Power plant-scale roller mill.* The horizontal LM 19.2D roller mills (Loesche  
156 GmbH, Germany) are used for comminution of wood pellets at AMV. Larger  
157 LM 23.2D roller mills are operated at AVV. A horizontal roller mill com-  
158 prises of 2-6 conical rollers which are hydraulically pressed onto a horizontal  
159 rotating grinding table [21]. The roller axis is inclined at  $15^\circ$  to the table,  
160 and the axes of the rollers and table do not intersect, as shown in Figure 4.

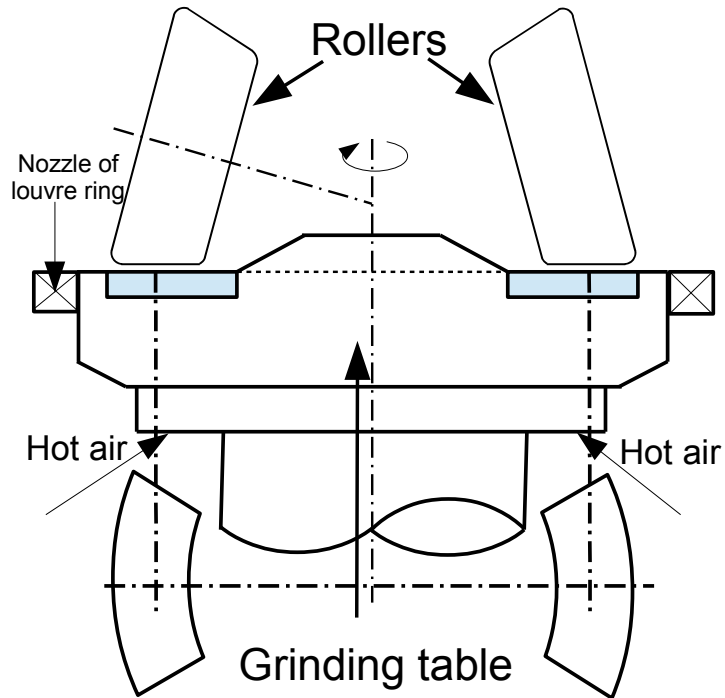


Figure 4: A schematic representation of a power plant-scale roller mill [21–23].

161 Feedstock is directed onto the center of the table and is thrown outward  
 162 by rotation under the rollers and into a rising air flow at the periphery which  
 163 is directed by means of a louvre ring that surrounds the grinding table and  
 164 conveys the air flow to the classifier. Fine fuel particles pass with the air flow  
 165 through an integral rotary classifier, whereas coarse fuel particles remain on  
 166 the feed table [21]. Throughput of the horizontal roller mills is up to  $70 \text{ t h}^{-1}$ .

167 *Laboratory-scale hammer mill.* In this study, Andritz 650-450 hammer mill  
 168 (Andritz GmbH, Germany) was used. A hammer mill consists of hammers

169 installed on a rotating disk which is enclosed within a liner [24]. Feedstock  
170 is drawn into the mill, and ground by the impact between hammers and the  
171 wall, as shown in Figure 5.

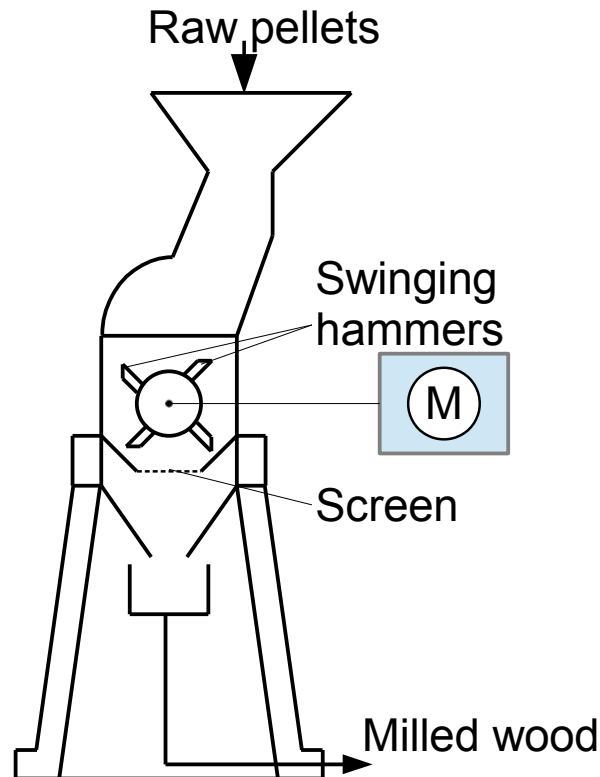


Figure 5: A schematic representation of a hammer mill [24].

172 The speed of the hammers produces kinetic energy that is dissipated on  
173 the material, leading to its disintegration. Feedstock is hammered until it  
174 is small enough to pass through the screen, and then is removed by shov-  
175 els, augers, or a chain elevator [25]. The hammer mill at HEV has a drum  
176 diameter of 650 mm and a drum length of 450 mm with four hammer shafts  
177 (fifteen hammers per shaft). Throughput of the mill is up to  $10 \text{ t h}^{-1}$ .

178 *Laboratory-scale roller mill.* A laboratory-scale roller mill at TU Clausthal  
179 was applied in this study, which is designed as a roller table mill with a single  
180 roller. A sketch [26] of the roller mill at TU Clausthal is shown in Figure 6:

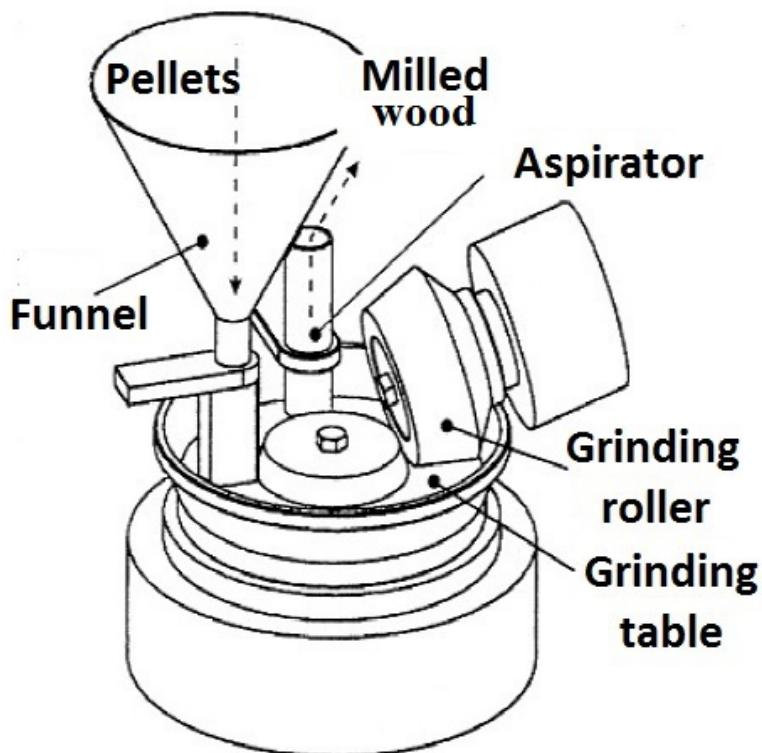


Figure 6: A schematic representation of a laboratory-scale roller mill at TU Clausthal [26].

181 The grinding table is circular and driven by an electrical motor. The  
182 conical grinding roller is placed over the grinding table and mounted at the  
183 lever system with a spring. The adjustable stop limits the lever's movement  
184 to avoid contact between the roller and the table. The feeding system, con-  
185 sisting of a funnel and shaft, is mounted opposite to the roller. The distance  
186 between the table bottom and the shaft outlet can be varied to control the



187 feeding rate. The tube positioned behind the roller serves to discharge the  
188 lignocellulosic materials. The mill is equipped with transducers for adjusting  
189 the torque, the grinding force and the gap between the roller and the table  
190 bottom [26]. The table diameter is 150 mm and the width is 42 mm, the mid-  
191 dle roller diameter is 100 mm with a roller width of 40 mm. The maximal  
192 roller inclination is  $15^\circ$ , the maximal motor power is 5.5 kW, and table rev-  
193 olutions vary from 5 to  $150 \text{ min}^{-1}$ . Throughput of the laboratory-scale roller  
194 mill is between 11 and  $14.7 \text{ kg h}^{-1}$ .

195 *Rotorprobe sampling method.* The material, comminuted in both the laboratory-  
196 and the power plant-scale mills, was sampled from the mills exit tubes using  
197 a rotorprobe and a vacuum cleaner. The rotorprobe method is described in  
198 EN ISO 9931:1991. Samples were extracted using a sampling probe consist-  
199 ing of four nozzles; each nozzle extracts from an equally sized area of the  
200 pipeline to ensure uniform collection.

201 *Vacuum cleaner sampling method.* A vacuum cleaner entrains pulverized ma-  
202 terial from a pipeline, which supplies fuel to the burners. A vacuum cleaner  
203 hose was placed perpendicular to the direction of flow. The principle of the  
204 vacuum cleaner sampling is shown in Figure 7.

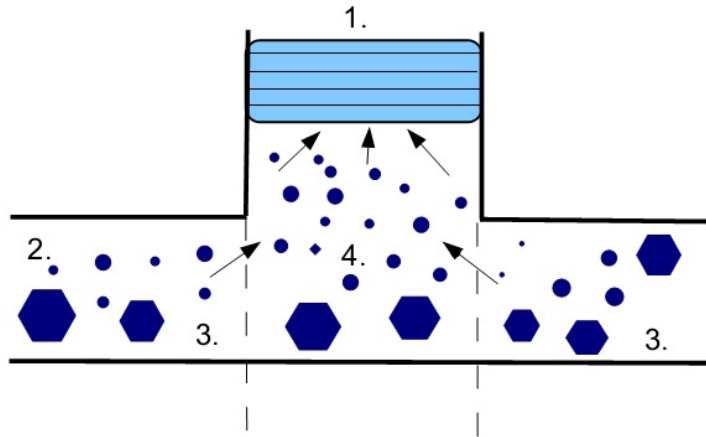


Figure 7: Vacuum cleaner sampling method: (1) vacuum cleaner, (2) particles flow in the pipe, (3) sector of flow before and after sampling and (4) sampling sector.

205 *Filtering.* In hammer mills, air is drawn at the top of the mill to cool the  
 206 mill components and draw the milled material through the screens into the  
 207 outlet hopper. The air and fine fuel particles are drawn to the air exhaust  
 208 via a bag filter. The remaining coarse material is collected at the bottom  
 209 of the outlet hopper. Both coarse and fine fractions are discharged from the  
 210 mill using screw feeders.

211 *Pellets.* Table 1 lists the pellet samples from the comminution on the hammer  
 212 and roller mills.

Table 1: Sample specification, comminution parameters and composition of milled pellets.

Identifier	DE 1658-4	DE 1663-16	VF 21 4, VF 21 6, VF 22 4, VF 23 4	VF 21 8, VF 33 8
	mill type	Loesche roller mill LM 23.2 D	Hammer mill	Loesche roller mill LM 19.2 D
power plant	AVV	HEV	AMV	
sampling method	*r	*f	*r	*r, *vc
mill screen size		2 mm		
rotating classifier	1		1	
energy consumption	10 kWh t <sup>-1</sup>	29 kWh t <sup>-1</sup>	8 kWh t <sup>-1</sup>	
bulk density of pellets	1.29 g cm <sup>-3</sup>	1.31 g cm <sup>-3</sup>	-	
moisture	5.2 %	7.8 %	6.3-6.7 %	
composition	10 % softwood + 90 % hardwood		50 % softwood + 50 % hardwood	

\*r - rotorprobe, \*f - filtering, \*vc - vacuum cleaner

213 The 8 mm pellets were produced in Latvia (LatGran), and used to  
 214 make DONG Energy samples (DE 1658-4 and DE 1663-16), as shown in  
 215 Table 1. The identifiers DE 1658-4 and DE 1663-16 include the company  
 216 name (DONG Energy) which is followed by the sample number; 4 and 15  
 217 include the fourth and the sixteenth samples taken, respectively. Pellets con-  
 218 sist of 10 % hardwood and 90 % softwood, and were produced from 70 % fine  
 219 sawdust and 30 % coarse sawdust. A larger percentage of softwood contains  
 220 Scots pine (*Pinus sylvestris*), Norway spruce (*Picea abies*), European aspen  
 221 (*Populus tremula*), whereas a smaller percentage of hardwood consists of  
 222 birch (*Betula* spp) and alder (*Alnus* spp), according to the feedstock classi-  
 223 fication described in EN ISO 17225-1:2016. The age of the roundwood with  
 224 bark used for making pellets ranged from 15 to 95 years. The particle size  
 225 distribution of the original sawdust prior to pelletization is shown in Table 2:

Table 2: Particle size distribution of the raw material used for making DE 1658-4 and DE 1663-16 samples. The particle size was determined by sieving.

mm	%
> 2.8	1.2
2.0-2.8	5.5
1.4-2.0	14.9
1.0-1.4	18.7
0.5-1.0	27.7
0.25-0.5	16.4
< 0.25	15.8

226 The 4 mm pellets were produced in Estonia (Heatlets), and were used  
 227 to make the AMV samples (VF 21 4, VF 21 6, VF 22 4, VF 23 4, VF 33 8,  
 228 VF 21 8), as shown in Table 1. The identifiers 21, 22, 23, and 33 are sample  
 229 numbers; the numbers 4, 6, and 8 represent the mass flow rate ( $\text{kg s}^{-1}$ ) in  
 230 the pipelines running from the mill. The numbers 2 and 3 in parentheses  
 231 found in abbreviations VF (2)3 4 and VF (3)3 8, indicate the second and  
 232 the third mill of the power plant. The pellets consist of 50% alder (*Alnus*  
 233 *spp*) and 50% softwood (Scots pine 45%, Norway spruce 5%), and were  
 234 manufactured from 75% fine sawdust and 25% coarse sawdust, according to  
 235 the feedstock classification described in EN ISO 17225-1:2016. The particle  
 236 size distribution of the raw feedstock used to make the VF pellets is shown  
 237 in Table 3:

Table 3: Particle size distribution of the raw material (VF 21  $8 \text{ kg s}^{-1}$  and VF 33  $8 \text{ kg s}^{-1}$ ) before pelletization determined by sieving.

mm	%
> 3.15	1.92
2.8-3.15	0.08
2.0-2.8	2.32
1.4-2.0	76.36
0-1.4	19.3

238 **5. Results**

239 *5.1. Comparison of the particle size characterization methods*

240 In this work, both sieving and 2D dynamic imaging were used. There-  
 241 fore, it is instructive to compare the samples using both methods. Samples  
 242 (DE 1658-4, DE 1663-16, VF 21  $8 \text{ kg s}^{-1}$ , and 33  $8 \text{ kg s}^{-1}$ ) of the pulverized  
 243 biomass were measured using the CAMSIZER and presented as a cumula-  
 244 tive distribution, based on volume ( $Q_3$ ), over the  $x_{Ma,min}$  diameter. The 2D  
 245 dynamic imaging data and the sieving data are compared in Figure 8:

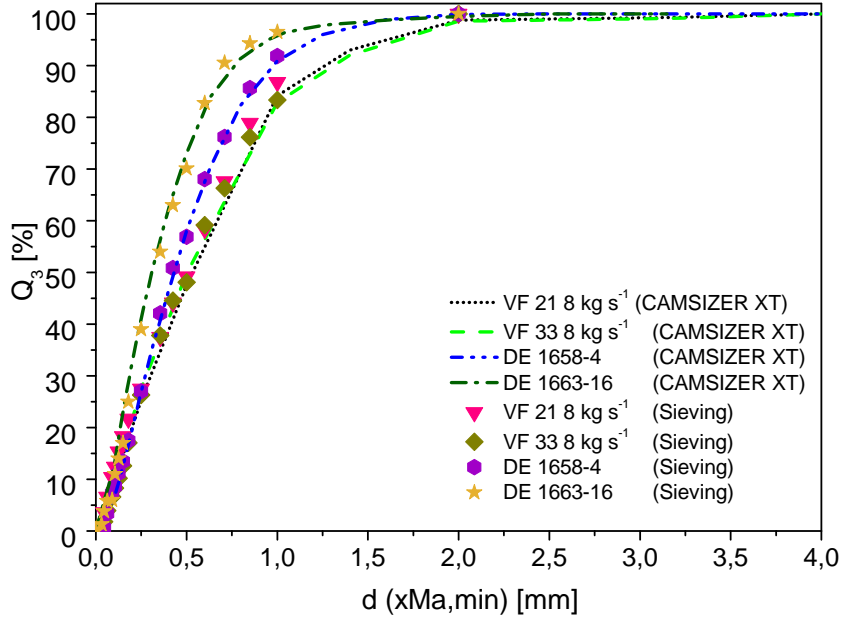
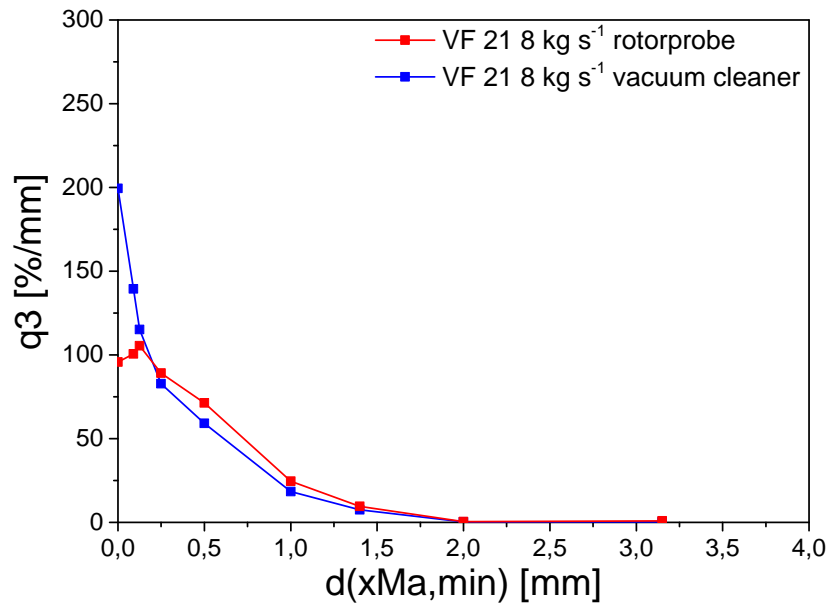


Figure 8: Cumulative particle size distribution  $Q_3$ , based on volume, for DE 1658-4, DE 1663-16, VF 21  $8 \text{ kg s}^{-1}$ , and VF 33  $8 \text{ kg s}^{-1}$  samples milled in the power plant-scale roller- and laboratory-scale hammer mills, and characterized by sieving and 2D dynamic imaging.

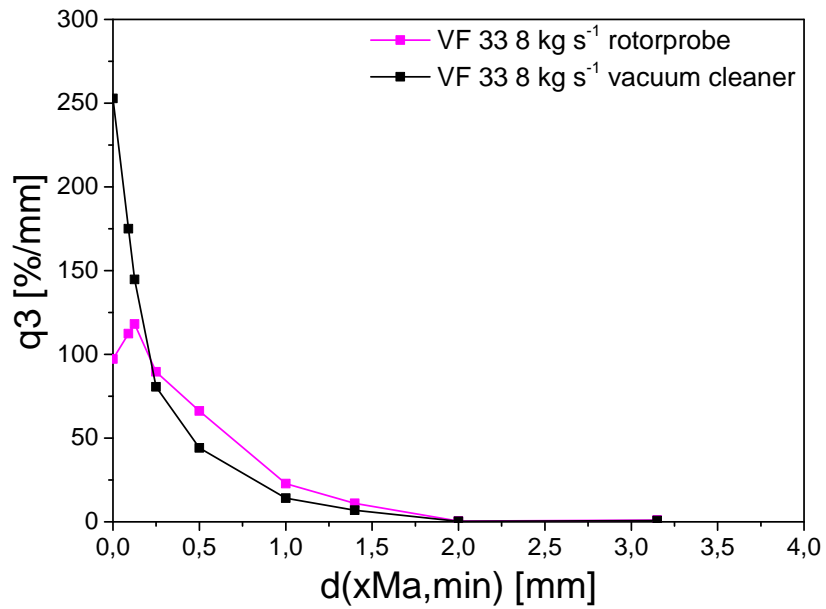
246 Sieving and 2D dynamic imaging produced very similar size distribu-  
 247 tions, as shown in Figure 8. The particle size analysis indicated that samples  
 248 DE 1658-4 and DE 1663-16 contained a larger fraction of small particles  
 249 compared to pulverized biomass obtained after milling the AMV pellets.  
 250 The comparable results obtained using both sizing techniques justify the ap-  
 251 plication of sieving, when large sample quantities are analyzed, whereas 2D  
 252 dynamic imaging analysis is more applicable when additional information  
 253 about geometrical parameters (length, width, etc.) and shape is required.

254 *5.2. Effect of sampling method on particle size and shape*

255 The effect of sampling method on particle size and shape was inves-  
256 tigated using samples VF 21  $8 \text{ kg s}^{-1}$  and 33  $8 \text{ kg s}^{-1}$ . The samples were  
257 collected using a vacuum cleaner and a rotorprobe mounted on horizontal  
258 piping. Collected particles were subsequently characterized by 2D dynamic  
259 imaging. Figure 9 shows that the sampling method affects the measured par-  
260 ticle size distribution for both samples. The samples collected by the vacuum  
261 cleaner showed a large fraction of fines, whereas the rotorprobe samples con-  
262 tained coarser particles. Since the vacuum cleaner has a larger inlet and the  
263 operator can easily move a vacuum cleaner hose inside the pipeline, the large  
264 particles do not entrain properly. Meanwhile, by placing the probes perpen-  
265 dicular to the direction of flow, the rotorprobe has a greater cross section to  
266 collect pulverized wood particles. Therefore, a more representative sample  
267 is expected from the rotorprobe sampling. However, the flow restrictions in  
268 the inlets and cyclone, which was originally designed for coal, may have led  
269 to the collection of coarser particles.



9(a): Sample VF 21 8 kg s<sup>-1</sup>



9(b): Sample VF 33 8 kg s<sup>-1</sup>

Figure 9: Influence of sampling method on the particle size distribution for VF 21 8 kg s<sup>-1</sup> and VF 33 8 kg s<sup>-1</sup> samples. The 2D dynamic imaging is used for particle sizing.

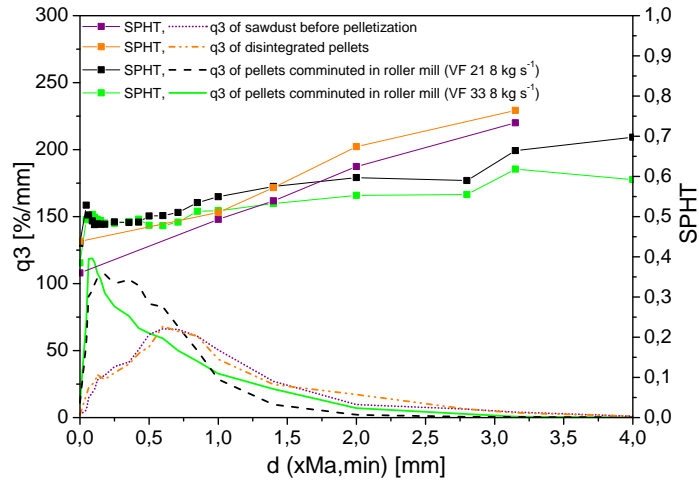


270 *5.3. Effect of pelletization and secondary milling on particle size*

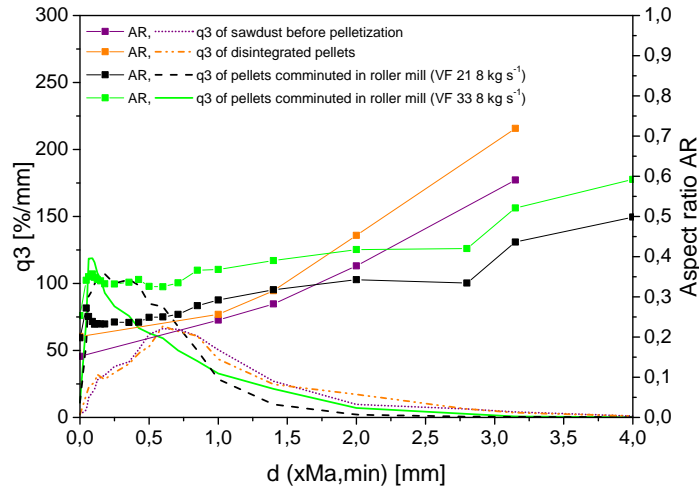
271 Disintegration of 8 mm LatGran pellets was carried out in deionized  
272 water for 10 min, followed by drying at 40°C for 4 h in an oven desiccator.  
273 Figure 10 shows the particle size distribution of sample VF 33 8 kg s<sup>-1</sup> before  
274 pelletization, disintegrated pellets and samples were collected after under-  
275 going secondary comminution on the roller mill. It is thereby possible to  
276 quantify the effect of pelletization and secondary comminution on particle  
277 size. Figure 10 indicates that the particle size distributions of the sawdust  
278 and the disintegrated pellets are similar. Thus, the pelletization process does  
279 not appear to modify the sizes of the component particles. However, as also  
280 shown in Figure 10, the differences between the particle frequency distribu-  
281 tions of the disintegrated pellets and the pellets comminuted on the roller  
282 mill are large. Secondary comminution step results in a further reduction  
283 of the original sawdust particle size by more than 40%. In addition, the  
284 particle size of pulverized wood can be affected by the sampling method and  
285 the disintegration process of pellets.

286 The sphericity (mean SPHT of all samples = 0.56) and the aspect ratio  
287 (mean AR of all samples = 0.51) of the comminuted pellets indicate that  
288 particles can be considered as cubic, as shown in Figure 10(a). The SEM  
289 microscopy shows that the largest particles indeed have a cubic shape (Fig-  
290 ure 11(c)), whereas smaller particles show various shapes with broken edges  
291 (Figure 11(d)). The original (before pelletization) sawdust particles and  
292 particles of the disintegrated pellets are elongated (mean SPHT of all samples  
293  $\approx 0.51$ ; mean AR of all samples  $\approx 0.53$ ), as shown in Figures 10(a) and 10(b).  
294 This observation was confirmed by 2D dynamic imaging. Light microscopy

295 confirmed that particles from the original sawdust as well as those in the  
296 disintegrated pellets displayed elongated shapes with small aspect ratios, as  
297 shown in Figures 11(a)-11(b).

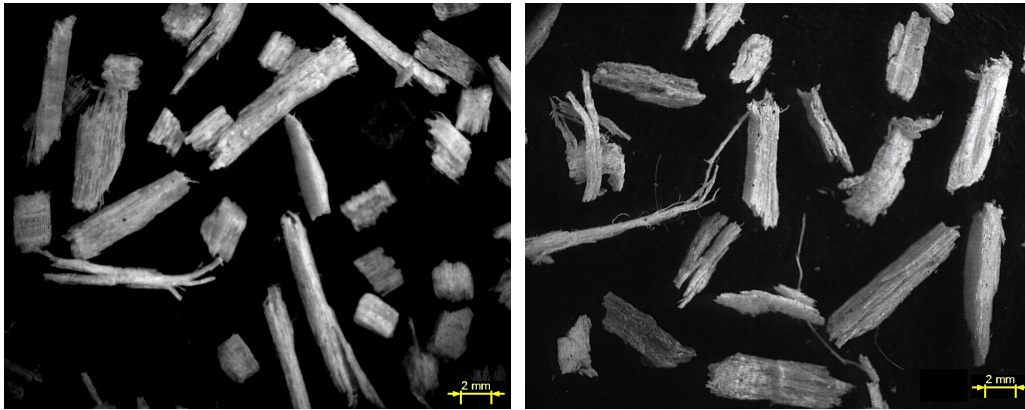


10(a): Sphericity

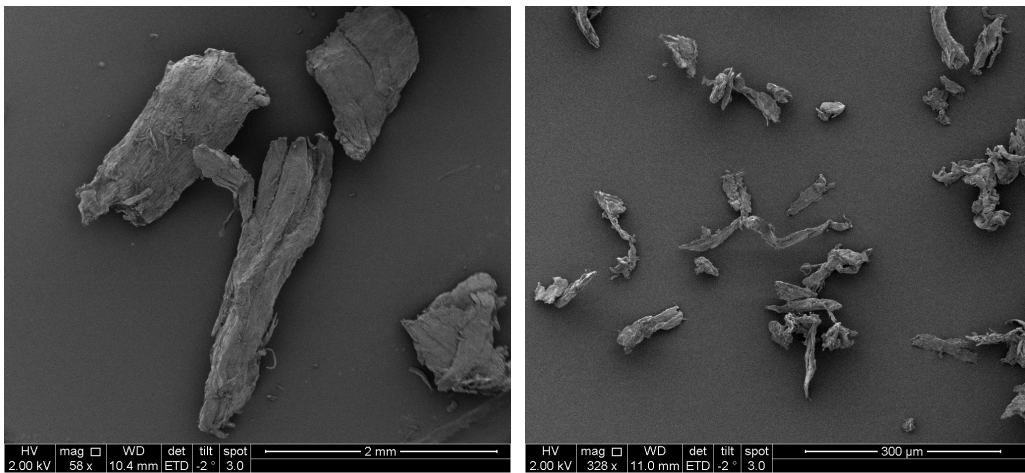


10(b): Aspect ratio

Figure 10: Particle size distribution  $q_3$ , based on volume, for  $VF\ 33\ 8\ \text{kg}\ \text{s}^{-1}$  and  $VF\ 21\ 8\ \text{kg}\ \text{s}^{-1}$  samples comminuted in the power plant-scale roller mill, original sawdust samples before pelletization and disintegrated pellets; shape factors (sphericity, aspect ratio) determined by 2D dynamic imaging.



11(a): Sawdust particles before pelletization    11(b): Particles from disintegrated pellets



11(c): VF 21  $8 \text{ kg s}^{-1}$  pellets (0.71-1 mm)    11(d): VF 21  $8 \text{ kg s}^{-1}$  pellets ( $< 0.18 \text{ mm}$ )

Figure 11: Light microscopy images of (a) sawdust before pelletization, (b) disintegrated pellets, and SEM images after comminution in the power plant-scale roller mill ( $\text{VF } 21 \text{ } 8 \text{ kg s}^{-1}$ ) and manually separated in two fractions (c) 0.71-1 mm and (d)  $< 0.18 \text{ mm}$ .

298        Typically, the sphericity and the aspect ratios of the original sawdust,  
 299 disintegrated pellets and comminuted pellets increase with particle size, in-  
 300 dicating that particles become more spherical and less elongated as their size

301 increases. However, the results from particles  $> 2$  mm were to be considered  
302 as non-representative in terms of shape description because the population  
303 of this fraction was too small.

#### 304 *5.4. Influence of mill type on particle size and shape*

305 Bond [12] concluded that biomass type has a greater impact on parti-  
306 cle shape than mill type. Rose [14] indicated that particle size and shape  
307 are mainly affected by mill type. In the present study, wood pellets were  
308 comminuted in roller- and hammer mills. Different types of wood pellets  
309 were comminuted on a roller mill to investigate the impact of feedstock and  
310 operational parameters of the mill on particle size and shape.

311 In Figure 12, the differences in particle size of pellets comminuted in  
312 the roller mill (DE 1658-4, VF 21 8 kg s<sup>-1</sup>, and VF 33 8 kg s<sup>-1</sup>) and in the  
313 hammer mill (DE 1663-16) are notable. Comminution in the hammer mill  
314 produced a larger fraction of fine particles, whereas comminution in the roller  
315 mill generated a more homogeneous product containing longer particles. The  
316 differences in particle size between samples DE 1658-4, VF 21 8 kg s<sup>-1</sup>, and  
317 VF 33 8 kg s<sup>-1</sup>, comminuted in the roller mills at AMV and AVV, are also  
318 substantial.

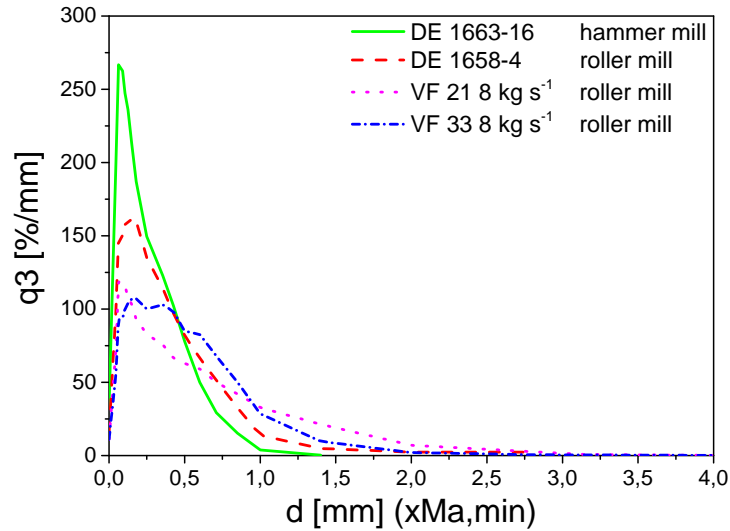


Figure 12: Particle frequency distribution  $q_3$ , based on volume, for DE 1658-4, DE 1663-16, VF 21  $8 \text{ kg s}^{-1}$ , and VF 33  $8 \text{ kg s}^{-1}$  samples milled in the power plant-scale roller- and laboratory-scale hammer mills, and characterized by 2D dynamic imaging.

319        The primary cause for the particle size differences among samples milled  
 320 in the roller mill are: pellet wood composition and differences in the classi-  
 321 fiers of the mills. The comminution in the roller and hammer mills led to  
 322 similar shaped-particles. The particles were rectangular ( $\text{SPHT} \approx 0.5\text{-}0.7$ );  
 323 the aspect ratios were similar at  $\text{AR} = 0.3$ . Symmetry and convexity of the  
 324 particles obtained by milling using either the hammer- or roller mill were also  
 325 similar. The comminution in both mills did not cause particle breakage, and  
 326 led to symmetrical polygonal particles containing holes ( $\text{Symm} = 0.7\text{-}0.9$ ;  
 327  $\text{Conv} \approx 0.95$ ), as shown in Figures 13(c)-13(d). Also the SEM microscopy  
 328 indicates that the differences in particle shape were small, as shown in Fig-

329 ure 14. Thus, the particles had similar shapes independent of mill type and  
 330 particle size.

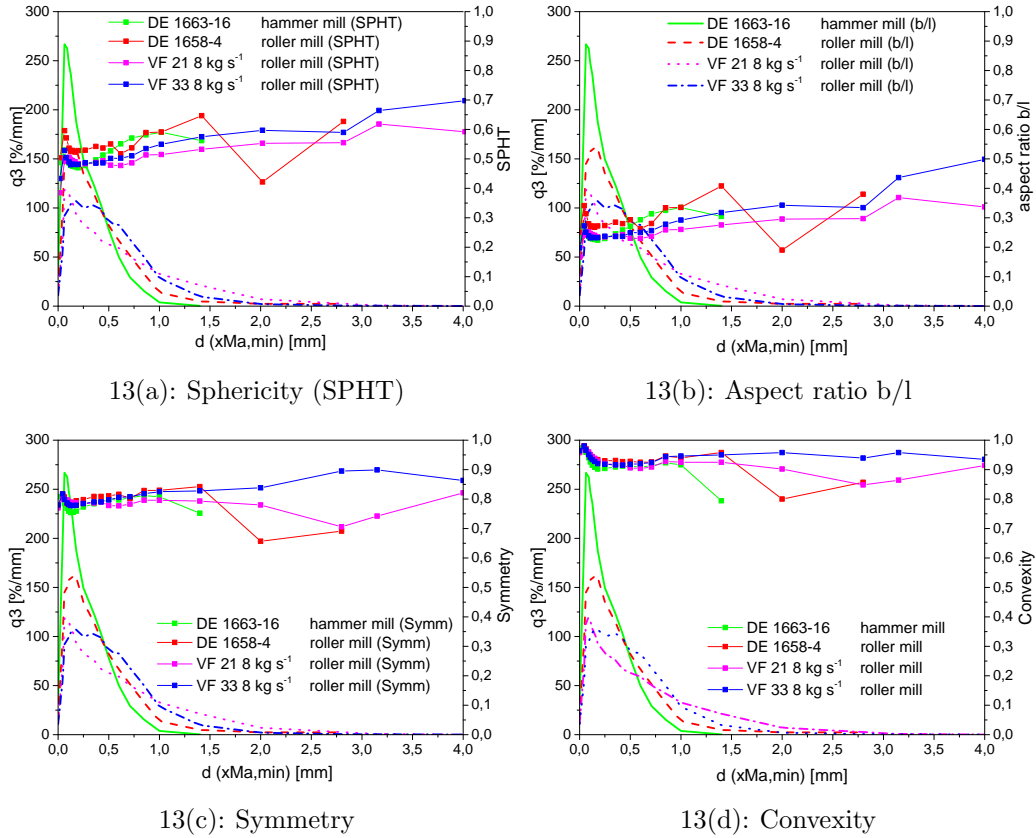
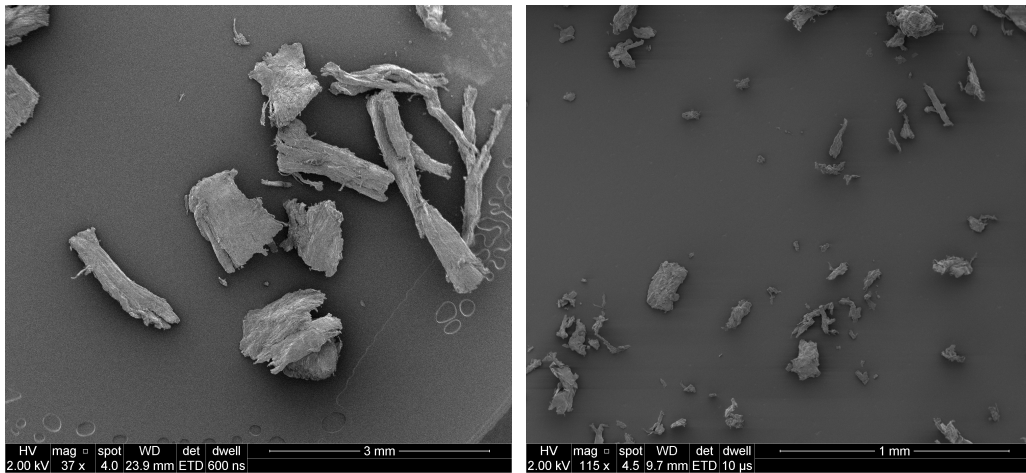
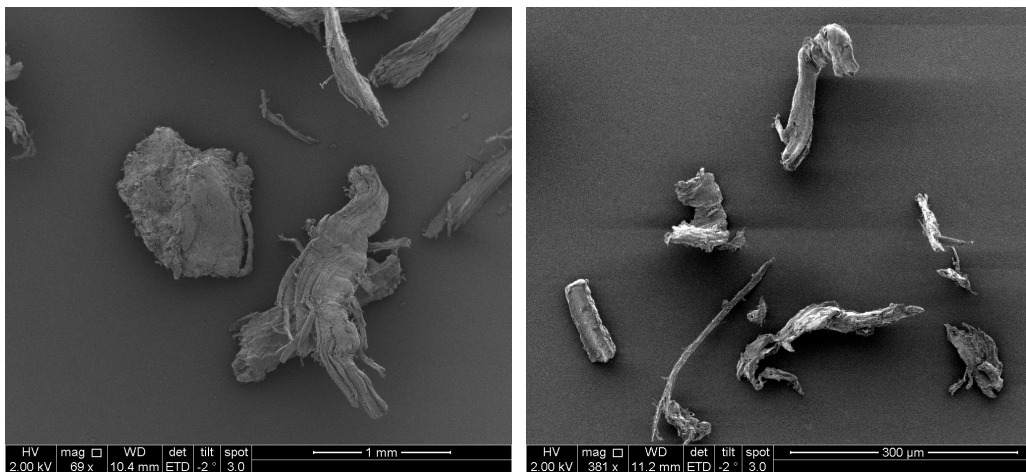


Figure 13: Shape factors (sphericity, aspect ratio  $b/l$ , symmetry and convexity) and size frequency distribution  $q_3$ , based on volume, for DE 1658-4, DE 1663-16, VF 21 8 kg s<sup>-1</sup>, and VF 33 8 kg s<sup>-1</sup> samples comminuted in the power plant-scale roller- and laboratory-scale hammer mills, and characterized by 2D dynamic imaging.



14(a): Pellets DE 1658-4 (roller mill, 0.71-1 mm)      14(b): Pellets DE 1658-4 (roller mill, < 0.18 mm)



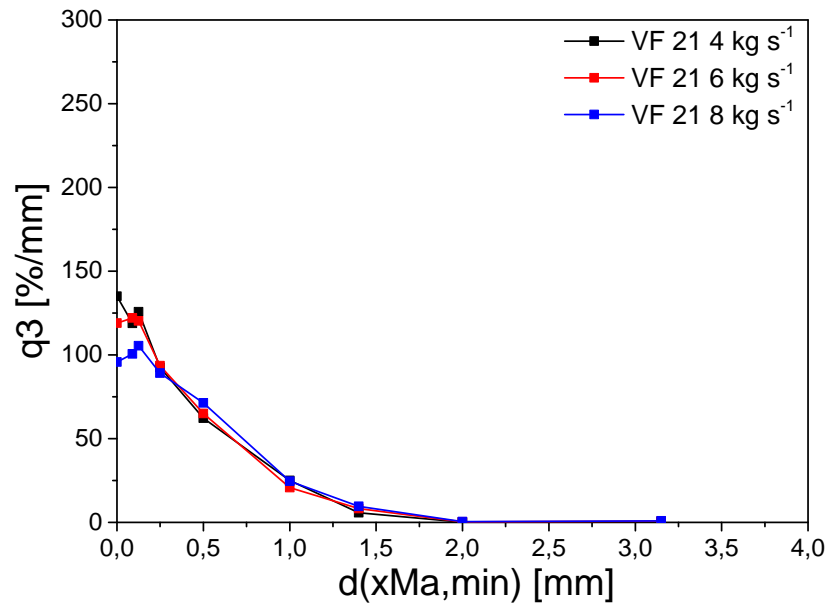
14(c): Pellets DE 1663-16 (hammer mill, 0.71-1 mm)      14(d): Pellets DE 1663-16 (hammer mill, < 0.18 mm)

Figure 14: SEM images of particles from pellets comminuted on power plant-scale roller and laboratory-scale hammer mills, and manually separated in particle size fractions < 0.18 mm and 0.71-1 mm.

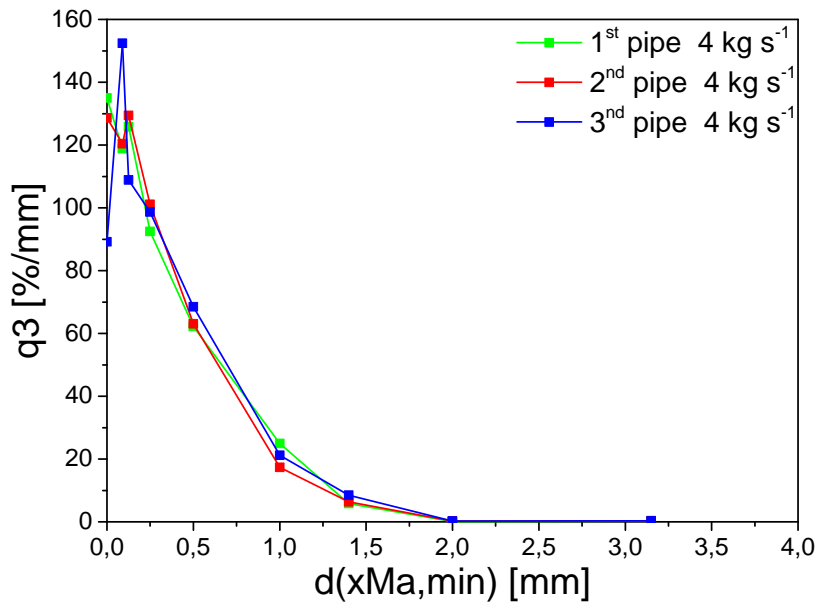


331 *5.5. Influence of mass flow rate on particle size and shape*

332 The impact of fuel mass flow rates in the pipelines, which supply the  
333 wood dust to the burners, was studied by examining powder flow rates of  
334 4, 6, and 8 kg s<sup>-1</sup>. The milled wood was delivered to the burner using four  
335 different pipes, but the particle size of the wood dust among the three output  
336 pipes was measured. It was reckoned that at a flow rate of 8 kg s<sup>-1</sup>, particle  
337 fragmentation in the pipeline may occur. However, Figure 15(a) shows that  
338 increasing biomass flow rate from 4 to 8 kg s<sup>-1</sup> did not significantly affect  
339 particle size. Differences in the milled wood particle size in the four pipes were  
340 expected to occur due to variations in throughput of the rotational classifier  
341 and due to different pressure drops caused by the pipe bends and length. In  
342 Figure 15(b), the particle size distributions of the wood transported at 4 kg  
343 s<sup>-1</sup> show that particle size was similar among the three output pipes.



15(a): Mass flow rate impact



15(b): Burner pipes impact

Figure 15: Particle size distribution of pellets milled in the power plant-scale roller mill (20) (a) different feedstock flow rates and (b) in different pipelines (21, 22, 23). The particles were sampled using the rotorprobe.

344 5.6. Impact of roller mill size on particle size and shape

345 A kilogram of VF 21  $8 \text{ kg s}^{-1}$  pellets was put into the funnel of the labo-  
346 ratory mill, as shown in Figure 6, which was operated at  $15^\circ$  roller inclination  
347 and 10 rpm. Figure 16 shows the particle size distribution after milling sam-  
348 ple VF 21  $8 \text{ kg s}^{-1}$  in the laboratory-scale mill and in the power plant-scale  
349 Loesche roller mill at AMV. It can be observed that the laboratory-scale  
350 mill at TU Clausthal provides comparable results to those obtained using  
351 the power plant-scale roller mill, currently operated by AMV, with respect  
352 to particle size distribution and particle shape. According to the conducted  
353 analysis, the results from the laboratory-scale roller mill well represented the  
354 changes in particle size and shape imposed by comminution in the power  
355 plant mill.

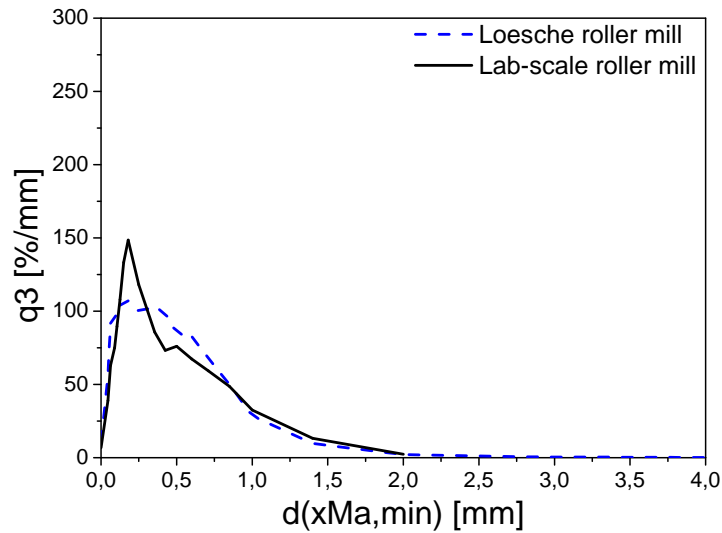


Figure 16: Particle frequency distribution  $q_3$ , based on volume, for VF 21  $8 \text{ kg s}^{-1}$  sample comminuted in the laboratory-scale and power plant-scale roller mills, and characterized by 2D dynamic imaging.

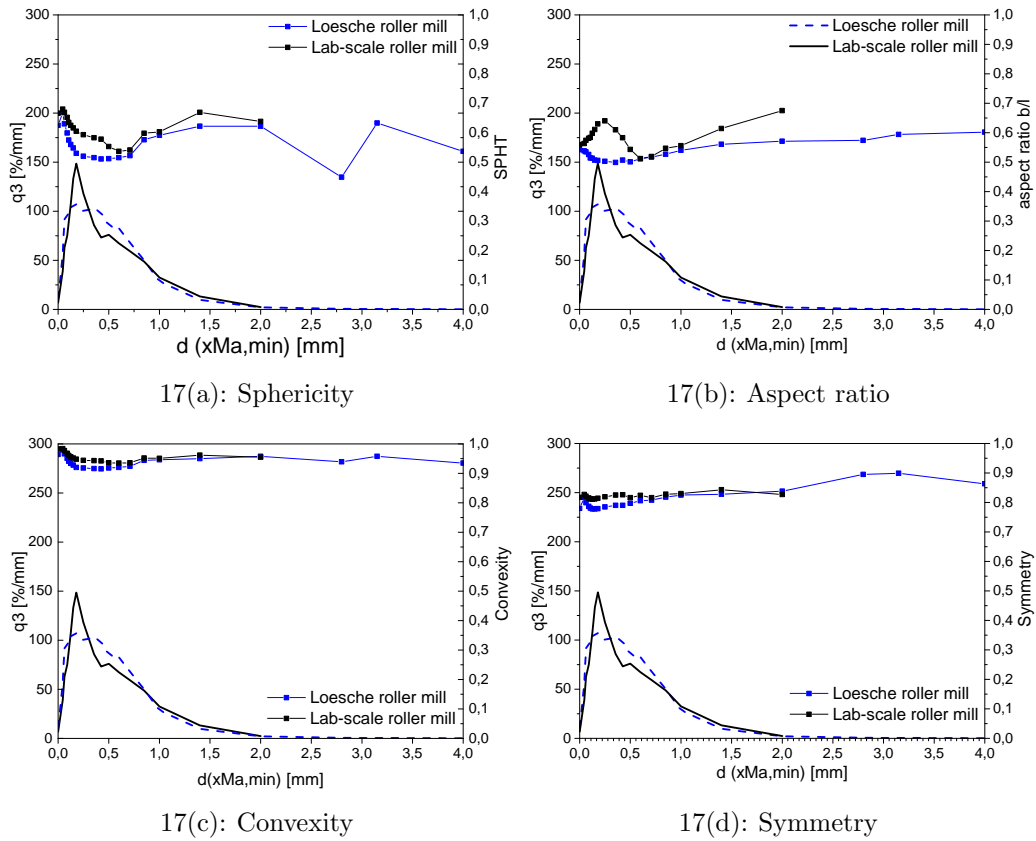


Figure 17: Shape factors (sphericity, aspect ratio  $b/l$ , symmetry and convexity) and size frequency distribution  $q_3$ , based on volume, for VF 21  $8 \text{ kg s}^{-1}$  sample comminuted in the laboratory-scale roller mill and the power plant-scale mill, and characterized by 2D dynamic imaging.

## 356 6. Discussion

357 The investigations showed only a small difference (less than 5%) in a  
 358 particle size of the original wood powder (used to produce the pellets) and the  
 359 powder obtained after disintegrating of the pellets. The results obtained from  
 360 material derived from the power plant-scale roller mills clearly demonstrated

361 that most pellets were broken down to sizes from 0.75 to 0.1 mm which are  
362 substantially smaller than sizes of original powder (sawdust) after milling.

363 The impact of different mill types on both particle size and shape was  
364 studied using the roller- and hammer mills. The results showed that mill type  
365 has the most significant influence on the size distribution of the pulverized  
366 wood. The analyzed hammer-milled samples contained a large fraction of fine  
367 particles compared to the roller-milled samples. The particle size was affected  
368 by sampling methods; the vacuum cleaner sampling was biased towards small  
369 particles. Further studies are required to determine the effect of sampling  
370 method on pulverized wood particle size and shape. The pellet samples  
371 from DONG Energy which contained a large percentage of softwood (90 %)  
372 produced finer particles after milling than the AMV pellets which were made  
373 out of a mixture of 50 % softwood and 50 % hardwood.

374 The shape of milled wood was only slightly influenced by the mill type.  
375 The results showed a small variation in sphericity, aspect ratio and convexity.  
376 The sphericity and aspect ratio for particle fractions of size  $< 2$  mm remained  
377 unaltered. For larger particles, the shape characterization does not provide  
378 statistically significant results due to small sample amounts. It was observed  
379 that longer particles were rectangular in shape and had more broken edges  
380 than their smaller counterparts.

381 The hammer and the roller mills require different energy inputs for con-  
382 ducting comminution. The input energy of the hammer mill was  $29 \text{ kWh t}^{-1}$   
383 whereas the roller mills required up to  $10 \text{ kWh t}^{-1}$  under full load. Thus,  
384 the roller mills are more energy efficient, confirming the results of Tamura et  
385 al. [27].

386 Pellets comminuted in a power plant roller mill were compared with the  
387 pellets comminuted in the laboratory-scale roller mill at TU Clausthal. The  
388 particle size and shape of milled wood, after milling the pellets either in the  
389 laboratory-scale or in the power plant Loesche roller mill, were similar. Thus,  
390 the results from the laboratory-scale mill represented well by the pilot plant  
391 size roller mill. This comparison was made for one sample only. Further  
392 systematic studies are needed to establish a confident relationship between  
393 the laboratory-scale and power plant-scale milling processes.

## 394 **7. Conclusion**

395 An experimental study was carried out to investigate the milling char-  
396 acteristics of biomass pellets milled in Danish power plants. Several samples,  
397 comminuted in hammer- and roller mills, were analyzed to establish a rela-  
398 tionship between mill type, pellet wood composition (softwood/hardwood)  
399 and the size and shape of milled wood. The particle size and shape charac-  
400 terization was conducted using sieving and 2D dynamic imaging.

401 The mill type and pellet wood composition strongly affected particle size  
402 and to a lesser degree particle shape. The secondary comminution of pellets  
403 in the hammer and roller mills produced milled wood that contained particles  
404 from 0.75 to 0.1 mm which are substantially smaller than the original sawdust  
405 particles used in pelletizing. The secondary comminution in the power plant  
406 mills produced rectangular particles. No variations in particle size with the  
407 milled wood flow rate were observed. No fragmentation of particles in the  
408 pipelines, which transport the milled wood to the burners, occurred.

409 Hammer mills were shown to require more energy than roller mills. The

410 comminution in the roller mill generated more coarse particles ( $> 0.5$  mm)  
411 than milling in the hammer mill.

412 The pellets comminution, in the Loesche power plant-scale roller mill  
413 and in the laboratory-scale roller mill, resulted in very similar particle size  
414 distributions.

### 415 **Acknowledgements**

416 The authors would like to acknowledge the financial support received  
417 from the Danish Strategic Research Council (Grant Nr. DSF-10-093956),  
418 DONG Energy, Vattenfall and HOFOR. We would also like to thank the  
419 Wood Sciences Laboratory at Technical University of Munich for the help  
420 with the pellets comminution in the laboratory-scale hammer mill to test the  
421 repeatability of our results. Jarl Wallden from LatGran and Kalju Erras from  
422 Heatlets are acknowledged for helping with the preparation of wood mate-  
423 rial before pelletization. The authors thank DTU Combustion and Harmful  
424 Emission Control group for fruitful discussions. Jayme Currie and Associate  
425 Professor Sunkyu Park are acknowledged for the article proof reading.

426 **References**

- 427 [1] Saleh SB, Hansen BB, Jensen PA, Dam-Johansen K, Influence of  
428 Biomass Chemical Properties on Torrefication Characteristics, *Energy*  
429 *Fuels* 27 (2013) 7541–8.
- 430 [2] Spinelli R, Cavallo E, Facello A, Magagnotti N, Nati C, Paletto G,  
431 Performance and energy efficiency of alternative comminution principles:  
432 Chipping versus grinding, *Scan J Forest Research* 27 (2012) 393–400.
- 433 [3] Mandø M, Rosendahl L, Yin C, Sørensen H, Pulverized straw combus-  
434 tion in a low  $\text{NO}_x$  multifuel burner: Modeling the transition from coal  
435 to straw, *Fuel* 89 (2010) 3051–62.
- 436 [4] Momeni M, Yin C, Koer SK, Hansen TB, Jensen PA, Glarborg P, Exper-  
437 imental Study on Effects of Particle Shape and Operating Conditions on  
438 Combustion Characteristics of Single Biomass Particles, *Energy Fuels* 27  
439 (2012) 507–14.
- 440 [5] Momeni M, Fundamental Study of Single Biomass Particle Combustion.  
441 PhD thesis, Aalborg University (2012).
- 442 [6] Himmel M, Tucker M, Baker J, Rivard C, Oh K, Grohmann K, Com-  
443 minution of Biomass: Hammer and Knife Mills, *Biotech Bioeng Symp*  
444 15 (1985) 39–58.
- 445 [7] Paulrud S, Mattsson JE, Nilsson C, Particle and handling characteristics  
446 of wood fuel powder: effects of different mills, *Fuel Process Tech* 76  
447 (2002) 23–39.



- 448 [8] Paulrud S, Upgraded Biofuels - Effects of Quality on Processing, Han-  
449 dling Characteristics, Combustion and Ash melting. PhD thesis, Umeå  
450 University (2004).
- 451 [9] Schell DJ, Harwood C, Milling of Lignocellulosic Biomass, *Appl Biochem*  
452 *Biotech* 46 (1994) 159–69.
- 453 [10] Miao Z, Grift TE, Hansen AC, Ting KC, Energy requirement for com-  
454 minution of biomass in relation to particle physical properties, *Ind Crops*  
455 *Prod* 33 (2011) 504–13.
- 456 [11] Ogden C, Iteleji K, Richardson F, Morphological Properties and Break-  
457 age Behavior of Three Ground Biofeedstocks by Hammermilling, *Am*  
458 *Soc Agr Bio Eng Ann Int Meet* 8 (2009) 5150–60.
- 459 [12] Bond FC, Control particle shape and size, *Chem Eng* 61 (8) (1954)  
460 195–8.
- 461 [13] Heywood H, Powders in industry, *Soc Chem Ind* (1961) 25–6.
- 462 [14] Rose HE, Particle shape and surface area, *Powders Ind* (1961) 130–49.
- 463 [15] Obernberger I, *The Pellet Handbook. The production and thermal util-*  
464 *isation of biomass pellets, FSC Mixed Sources, 2010.*
- 465 [16] Saad ES, Mostafa ME, Analysis of Grain Size Statistic and Particle Size  
466 Distribution, *Waste Biomass Valor* 5 (2014) 1005–18.
- 467 [17] Williams O, Newbolt G, Eastwick C, Kingman S, Giddings D, Lester  
468 E and etc., Influence of mill type on densified biomass comminution,  
469 *Applied Energy* 182 (2016) 219–31.

- 470 [18] Stuess M, *Mechanische Verfahrenstechnik 1* (in German), Springer, 1992.
- 471 [19] Merkus HG, *Particle Size Measurements*, Springer, 2009.
- 472 [20] Tannous K, Lam PS, Sokhansanj S, Grace JR, Physical properties for  
473 flow characterization of ground biomass from Douglas Fir Wood, *Part*  
474 *Sci Technol* 31 (2012) 291–300.
- 475 [21] Alsop PA, *Cement Plant Operations Handbook*, Tradeship Publications  
476 Ltd, 2007.
- 477 [22] Schafer HU, Loesche mills for the cement industry, *ZKG Int* 56 (3) (2003)  
478 58–64.
- 479 [23] Reichert M, Gerold C, Fredriksson A, Adolfsson G, Lieberwirth H, Re-  
480 search of iron ore grinding in a vertical roller mill, *Mineral Eng* 73 (2015)  
481 109–15.
- 482 [24] Ghorbani Z, Masoumi AA, Hemmat A, Specific energy consumption for  
483 reducing the size of alfalfa chops using a hammer mill, *Biosys Eng* 105  
484 (2010) 34–40.
- 485 [25] Henderson P, *Agricultural process engineering*, Springer, 1976.
- 486 [26] Werner V, Zelkowski J, Schönert K, Lab-scale roller table mill for investi-  
487 gating the grinding behaviour of coal, *Energy Fuels* 22 (1999) 4292–300.
- 488 [27] Tamura M, Watanabe S, Kotake N, Hasegawa M, Grinding and combus-  
489 tion characteristics of woody biomass for co-firing with coal in pulverised  
490 coal boilers, *Fuel* 134 (2014) 544–53.